Earth's Future

RESEARCH ARTICLE
10.1029/2019EF001316

Key Points:
- In Australia, pasturelands have both low resistance and low resilience relative to other regions across the world
- Southern South America has the lowest resilience globally, which is indicative of slow vegetation recovery after a disturbance
- A total of 14.5% of global pasturelands experienced greening or browning trends, with the majority of these locations showing greening

Supporting Information:
- Supporting Information S1

Correspondence to:
R. Stanimirova,
rkstan@bu.edu

Citation:
Stanimirova, R., Arévalo, P., Kaufmann, R. K., Maus, V., Lesiv, M., Havlík, P., & Friedl, M. A. (2019). Sensitivity of Global Pasturelands to Climate Variation. *Earth's Future*, *7*. https://doi.org/10.1029/2019EF001316

Received 18 JUL 2019
Accepted 4 NOV 2019

Author Contributions:
Conceptualization: Radost Stanimirova, Paulo Arévalo, Robert K. Kaufmann, Myroslava Lesiv, Petr Havlík, Mark A. Friedl
Data curation: Radost Stanimirova, Paulo Arévalo
Formal analysis: Radost Stanimirova, Paulo Arévalo, Robert K. Kaufmann
Funding acquisition: Radost Stanimirova, Mark A. Friedl
Investigation: Radost Stanimirova, Paulo Arévalo
Methodology: Radost Stanimirova, Paulo Arévalo, Robert K. Kaufmann, Victor Maus, Myroslava Lesiv, Mark A. Friedl
(continued)

Sensitivity of Global Pasturelands to Climate Variation

Radost Stanimirova[1], Paulo Arévalo[1], Robert K. Kaufmann[1], Victor Maus[2,3], Myroslava Lesiv[2], Petr Havlík[2], and Mark A. Friedl[1]

[1]Department of Earth and Environment, Boston University, Boston, MA, USA, [2]Ecosystems Services and Management (ESM) Program, International Institute for Applied Systems Analysis (IIASA), Laxenburg, Austria, [3]Institute for Ecological Economics, Vienna University of Economics and Business (WU), Vienna, Austria

Abstract Pasturelands are globally extensive, sensitive to climate, and support livestock production systems that provide an essential source of food in many parts of the world. In this paper, we integrate information from remote sensing, global climate, and land use databases to improve understanding of the resilience and resistance of this ecologically vulnerable and societally critical land use. To characterize the effect of climate on pastureland productivity at global scale, we analyze the relationship between satellite-derived enhanced vegetation index data from MODIS and gridded precipitation data from CHIRPS at 3- and 6-month time lags. To account for the effects of different production systems, we stratify our analysis by agroecological zones and by rangeland versus mixed crop-livestock systems. Results show that 14.5% of global pasturelands experienced statistically significant greening or browning trends over the 15-year study period, with the majority of these locations showing greening. In arid ecosystems, precipitation and lagged vegetation index anomalies explain up to 69% of variation in vegetation productivity in both crop-livestock and rangeland-based production systems. Livestock production systems in Australia are least resistant to contemporaneous and short-term precipitation anomalies, while arid livestock production systems in Latin America are least resilient to short-term vegetation greenness anomalies. Because many arid regions of the world are projected to experience decreased total precipitation and increased precipitation variability in the coming decades, improved understanding regarding the sensitivity of pasturelands to the joint effects of climate change and livestock production systems is required to support sustainable land management in global pasturelands.

Plain Language Summary Pastures, which provide food for livestock, are the most extensive land use on the planet, and their productivity depends on the timing and amount of rainfall they receive. In this paper, we use data on vegetation productivity, rainfall, and land use in order to determine the ability of pastures to remain unaffected by a disturbance and the time required for pastures to recover following a disturbance. To determine the effects of rainfall on pastures, we analyze the relationship between productivity and rainfall at 3- and 6-month time intervals. We also take into account pasture management and whether pastures are located in dry or humid areas of the world. In dry regions, rain from the current season, rain from the last two seasons, and vegetation productivity from the previous growing season explain nearly 70% of current season vegetation productivity. Pastures in Australia are least capable of withstanding rainfall deficits, while pastures in Latin America recover more slowly after drought compared to other regions. Dry regions of the world are predicted to receive less rain less regularly in the coming decades, so improved understanding of the sensitivity of pastures to expected changes in rainfall will help support sustainable management of global pastures.

1. Introduction

More than a third of Earth's ice-free land surface is occupied by agriculture, of which nearly 70% is used as pastureland to support livestock (Foley et al., 2011). Although pasturelands occupy a disproportionate share of agricultural land, their productivity, resilience, and resistance to climate change are much less well-studied relative to croplands (Foley et al., 2011; Ramankutty et al., 2002). Because these systems are important both ecologically and to local and global economies, incomplete understanding regarding the dynamics and vulnerabilities of pastureland ecosystems to the joint effects of climate and livestock production systems represents a key knowledge gap.

Project administration: Robert K. Kaufmann, Victor Maus, Myroslava Lesiv, Petr Havlík, Mark A. Friedl
Resources: Paulo Arévalo, Robert K. Kaufmann, Victor Maus, Mark A. Friedl
Software: Radost Stanimirova, Paulo Arévalo, Robert K. Kaufmann, Victor Maus
Supervision: Robert K. Kaufmann, Victor Maus, Myroslava Lesiv, Petr Havlík, Mark A. Friedl
Validation: Radost Stanimirova, Paulo Arévalo
Visualization: Radost Stanimirova, Paulo Arévalo
Writing - original draft: Radost Stanimirova, Robert K. Kaufmann, Mark A. Friedl
Writing – review & editing: Radost Stanimirova, Robert K. Kaufmann, Victor Maus, Myroslava Lesiv, Petr Havlík, Mark A. Friedl

Growing population and increasing affluence in developing nations are expected to increase global meat and milk consumption by 68% and 57%, respectively, by 2030 relative to consumption in 2000 (Steinfeld & Gerber, 2010). In the era of climate change, our ability to satisfy increased demand for meat and dairy while decreasing the resulting environmental impact depends on pastureland sensitivity to both climate and livestock management. Quantifying the relationships among pastureland productivity, climate, and livestock production systems is therefore important to support forecasts regarding how ongoing changes in climate may lead to grassland feed shortages and pastureland degradation and desertification. Moreover, in order to meet the UN Sustainable Development Goals, improved understanding of the processes and thresholds that lead to land degradation in pastureland systems is required (Keesstra et al., 2016).

Precipitation is the dominant climatic control on grassland productivity (Knapp & Smith, 2001; Sala et al., 2012). From desert grasslands to mesic prairies, field-based studies show that mean annual precipitation accounts for up to 90% of interannual variation in aboveground net primary productivity (ANPP) (Del Grosso et al., 2008; Guo et al., 2012; Sala et al., 1988). At seasonal time scales, vegetation productivity in arid and semi-arid systems is largely driven by seasonal weather regimes with secondary responses to lagged weather, at time scales that range from 1 month (Wu et al., 2015) to 2 years (Arnone et al., 2008). Because pasturelands are actively grazed by livestock, understanding and modeling their response to precipitation variation is challenging and has been described using both equilibrium and nonequilibrium ecological theory. In arid and semi-arid systems, in particular, evidence suggests that livestock density alters the long-term direction of structure and composition of grasslands, but appears to have a minor role in regulating yearly plant production and forage availability, which is primarily influenced by episodic precipitation events at seasonal time scales (Briske et al., 2003; Fuhlendorf et al., 2001; Illius & O'Connor, 1999).

Arid and semi-arid ecosystems occupy approximately 40% of the terrestrial surface (Reynolds et al., 2007) and account for approximately 40% of global net primary productivity (NPP) (Bunting et al., 2017; Wang et al., 2012). Rangeland-based livestock production systems, which occupy 65% of drylands, support livestock on the ANPP of natural vegetation (Asner et al., 2004; Gaitán et al., 2014). Because water limits the productivity of vegetation in arid and semi-arid ecosystems, the timing and duration of precipitation drive ecosystem function by controlling the amount of soil moisture available for plant uptake (Sala et al., 2012; Wilcox et al., 2017). Recent studies suggest that up to 66% of global land areas are experiencing drying (Huang et al., 2015), and precipitation events in arid and semi-arid regions are forecast to become shorter, less frequent, and less widespread in the coming decades (Huang et al., 2015; Reeves et al., 2014). If realized, these changes pose a significant threat to the sustainability of rangeland-based livestock production systems, especially in arid and semi-arid regions.

The United Nations' Food and Agriculture Organization (FAO) defines pastures as land permanently used for herbaceous forage crops. Pastures provide 48% of the biomass used by ruminants (e.g., bovines, sheep, and goats) across both rangeland-based and mixed crop-livestock systems and are therefore important to food security in many parts of the world (Herrero et al., 2013). In mixed systems, livestock consume a wide variety of feeds, and crop by-products and stubble provide more than 10% of animal food. Mixed crop-livestock systems account for the majority of grass consumption and provide 61% of the meat and 69% of the milk produced in both developed and developing countries (Herrero et al., 2013). Livestock in rangeland-based systems, on the other hand, depend almost exclusively on grass for feed, with more than 90% of dry matter derived from pasturelands with limited feed supplements (Robinson et al., 2011).

At regional to continental scales, several studies have used satellite data to quantify the impact of precipitation variability on grassland productivity (e.g., Lotsch et al., 2003; Seddon et al., 2016; Vicente-Serrano et al., 2013). However, most have not considered the potential for management practices to offset or exacerbate the impact of climate variability on pastureland production (Knapp et al., 2015; Sala et al., 2012; Wilcox et al., 2017). Including land use in such analyses provides a basis for separating the effects of livestock production systems from climatic drivers and could inform ecosystem management and policies. No study has examined the relationships among the resilience and resistance of pasturelands to both climate anomalies and livestock production systems at global scales. Further, few studies have estimated quantitatively the sensitivity of pastureland vegetation to precipitation at different time lags at global scale.

In this paper, we use observations (2003–2017) from a suite of precipitation, livestock, and remote sensing data sets to characterize and assess the spatially explicit sensitivity of global pasturelands located in

10.1029/2019EF001316

different livestock production systems to climate. We define *sensitivity* as the change in satellite-derived vegetation greenness that is generated by a change in precipitation (Huxman et al., 2004; Knapp et al., 2015; Sala et al., 2012). Specifically, we estimate both vegetation *resistance* (ability of pasturelands to withstand a disturbance) and *engineering resilience* (time required for pasturelands to return to set point after a disturbance) to variations in precipitation, as conditioned on livestock production system. We postulate that the geographic distribution, productivity, and sensitivity of global pasturelands depend on the combined effects of precipitation and the livestock production system (i.e., mixed crop-livestock and rangeland-based). Specifically, the objectives of the research we describe in this paper are as follows:

1. To quantify the resistance and resilience of arid/semi-arid and humid/sub-humid livestock production systems to climate.
2. To assess the nature and magnitude of short-term precipitation and vegetation anomalies in determining pastureland greenness in different climatic zones and livestock production systems.

As part of our analysis, we also evaluate overall trends in vegetation greenness in global pasturelands and investigate the form and magnitude of pastureland vegetation response to wet versus dry years.

2. Materials and Methods

2.1. Remote Sensing and Precipitation Data Sets

Repeated satellite observations across broad spatial scales have been used as indicators of pastureland health and pastureland response to climate and anthropogenic drivers of change (Asner et al., 2004). For this work, we used time series of the enhanced vegetation index (EVI), which is correlated with the fraction of photosynthetically active radiation absorbed by plant canopies and vegetation biomass (Asrar et al., 1984; Myneni et al., 1995; Zhou et al., 2003), as a surrogate for vegetation productivity. Because EVI is closely related to ANPP, the magnitude and seasonality in EVI provide good indicators of forage availability (Gaitán et al., 2014). EVI is a measure of the aggregate response of pasturelands to both climate variability and grazing. Given that yearly plant production is often controlled by precipitation rather than grazing (Ellis & Swift, 1988; Briske et al., 2003; Fernandez-Gimenez & Allen-Diaz, 1999) and because spatially explicit grazing data are not available at global scale, we analyzed the response of pasturelands to precipitation explicitly recognizing that they may be grazed.

To evaluate the sensitivity of pastureland productivity to precipitation, we used gridded monthly precipitation data from the Climate Hazards Group InfraRed Precipitation Station (CHIRPS) data at 0.05° spatial resolution (Funk, Verdin, et al., 2015) and Collection 6 MODIS monthly EVI data (MOD13C2), also at 0.05° spatial resolution (Didan, 2015) from 2003 to 2017. Using the MOD13C2 monthly vegetation index quality flags, we limited the effect of clouds and atmospheric constituents on the EVI time series (for more details, see supporting information Table S2). Further, to exclude artifacts introduced by soil background and snow, we excluded EVI values less than 0.1 (Wu et al., 2015; Zhou et al., 2003). CHIRPS is a quasi-global rainfall data set spanning 50°S to 50°N across all longitudes. By utilizing high resolution (0.05°) satellite observations of global precipitation climatology in addition to physiographic indicators and gauge data, CHIRPS provides gridded precipitation data with good quality and coverage in data sparse regions (Funk, Peterson, et al., 2015) that compares favorably against the most widely used global precipitation data sets: the Climate Research Unit (CRU) time series and WorldClim (Funk, Peterson, et al., 2015).

2.2. Global Pastureland Map

We combined two sources of information to create a global map of pasturelands. First, we used the MODIS Collection 6 Land Cover Product (MCD12Q1) at 500 m spatial resolution (Sulla-Menashe et al., 2019) to restrict our analysis to locations belonging to the following land cover classes: closed shrublands, open shrublands, woody savannas, savannas, grasslands, barren or sparsely vegetated, and cropland/natural vegetation mosaic. To be conservative, we retained only those grid cells that were classified as one of the abovementioned land cover classes across all 15 years. Second, we used the map of global pasturelands circa 2000 created by Ramankutty et al. (2008), which blends coarse spatial resolution agricultural inventory data from the UN Food and Agriculture Organization (FAOSTAT) with land cover data derived from MODIS (Friedl et al., 2010). Specifically, we used Ramankutty et al.'s (2008) map to identify 5′ grid cells with 60% or more pastureland cover. We used Ramankutty et al. (2008) product since it provides the most conservative estimates of pastureland area when compared to other products because it considers only permanent pastures (Fetzel et al., 2017). We then intersected these two data sets to create a gridded map of pasturelands where each grid cell met two criteria: (1) stable land cover through time belonging to one of the seven MODIS Land Cover classes identified above and (2) possessing more than 60% pasture by area according to Ramankutty et al. (2008).

Following Robinson et al. (2018), pastureland areas were divided into two agroecological zones (arid/semiarid and humid/sub-humid), two livestock production systems (rangeland-based: defined as having minimal crop-based agriculture, and crop-livestock: defined as rainfed cropping combined with livestock production), and five different geographic regions (Africa, Asia, Australia, North America, and Latin America) (https://doi.org/10.7910/DVN/WPDSZE). We excluded Europe where pasturelands are not extensive. Following the regional stratification established by Herrero et al. (2013) we defined Latin America as including Mexico, Central America, and South America. This design identified 20 distinct geographic units, which were further subdivided into four seasons resulting in 80 different study units for the final model specification (Figure 1). We selected 30% of grid cells via random sampling (without replacement) from each of the twenty different geographic units (Table S1). This proportional sampling scheme allowed for a fair comparison among regions with markedly different areas (see supporting information for more details on sampling strategy and Table S1 for the number of grid cells in each region represented by 30% sample). In addition, to support estimation of uncertainty in model results, we repeated the procedure 100 times, providing 100 sets of unique random samples is each study unit.

2.3. Panel Regression Model

To characterize the sensitivity of pasturelands to the joint effects of land use and climate, we estimated panel regression models to predict EVI at seasonal time scale. We used a panel regression-based approach because this method is well suited for (1) gridded time series that have relatively few observations (15 years) for a large number of pixels (Hsiao, 2014) and (2) a stratified sampling approach such as the one described above (see supporting information). Panel regression models have been previously used in similar contexts to study yield response to climate in croplands as well as the relationship between remotely sensed vegetation indices and climate (Lobell & Burke, 2010; Zhou et al., 2003). To perform this analysis, CHIRPS precipitation and MODIS vegetation index time series were co-registered and clipped to the pastureland mask described above. For each 0.05° grid cell, we calculated seasonal statistics (mean, min, max, and standard deviation) and seasonal standardized anomalies for precipitation and EVI (Equation (1)), which removed the effect of seasonality and reduced the impact of spatial autocorrelation in each climate zone and livestock production system (Hansen et al., 1999; Zhou et al., 2003):

$$Anomaly_{s(y)} = \frac{\overline{x}_{s(y)} - \overline{x}_{s(ref)}}{\sigma_{s(ref)}}, \tag{1}$$

where y is year, $\overline{x}_{s(y)}$ is the mean for a season (s) and year (y), $\overline{x}_{s(ref)}$ is the long-term mean for the same season, and $\sigma_{s(ref)}$ is the standard deviation for the same season. Prior to computing the standardized seasonal anomalies, monthly EVI data were averaged, and monthly precipitation values were summed to generate seasonal values for December/January/February (DJF), March/April/May (MAM), June/July/August (JJA), and September/October/November (SON). Because precipitation is highly variable at short time scales and vegetation does not respond to high frequency variation in weather, we have adopted this widely used aggregation approach in our study (e.g., Lotsch et al., 2003; Vicente-Serrano et al., 2013; Zhou et al., 2003).

Linear panel regression models were estimated for each season (s) and grid cell (i) as follows:

$$EVI_{is} = \alpha_{is} + \sum_{s=0}^{-2} \left(\beta 1_{is} {*} P_{is} + \beta 2_{is} {*} {P_{is}}^2\right) + \beta 3_{is} {*} EVI_{i(s-1)} + \epsilon_{is}, \tag{2}$$

where P is the standardized precipitation anomaly, $EVI_{i(s-1)}$ is the standardized EVI anomaly from the previous season, α, $\beta 1$, $\beta 2$, and $\beta 3$ are coefficients that were estimated using the fixed effects estimator, and ϵ is the model residual. The coefficients associated with precipitation ($\beta 1$ and $\beta 2$) capture drought sensitivity, and the coefficient associated with lagged EVI ($\beta 3$) captures the sensitivity of pasturelands to preceding

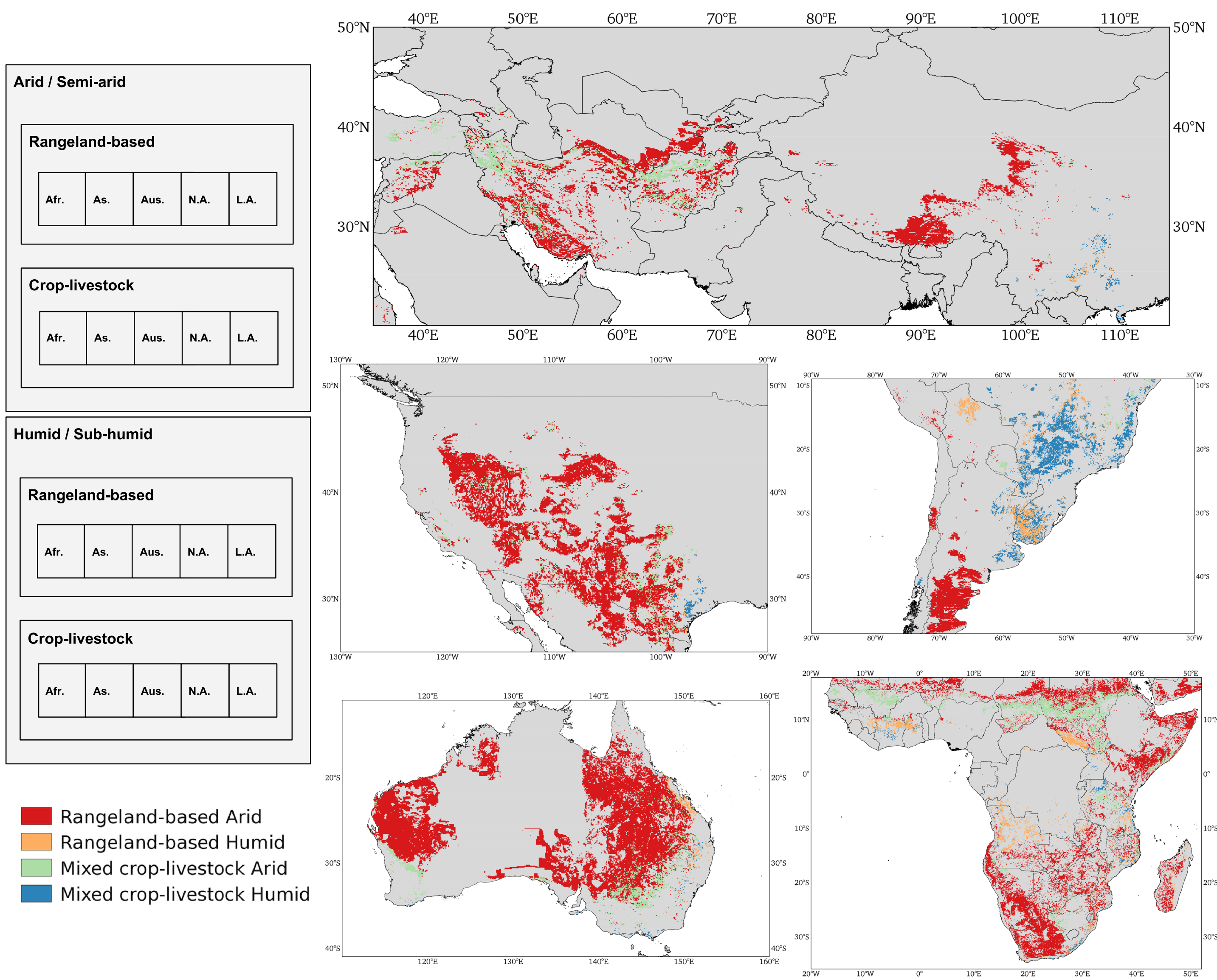

Figure 1. Global ruminant livestock production systems and sample design with two agroecological zones (arid/semi-arid and humid/sub-humid), two livestock production systems (rangeland-based and crop-livestock) and five different geographic regions (Africa [Afr.], Asia [As.], Australia [Aus.], North America [N.A.], and Latin America [L.A.]), resulting in 20 different study regions. The map has been adapted from Robinson et al. (2018), and it shows the applied pastureland mask. Rangeland-based arid pasturelands are shown in red, rangeland-based humid pasturelands are shown in orange, mixed crop-livestock arid pasturelands are shown in greed, and mixed crop-livestock humid pasturelands are shown in blue.

vegetation anomalies. Specifically, (1-β3) represents the rate at which EVI adjusts to the values implied by precipitation. In other words, coefficients β1 and β2 capture the drought resistance, whereas coefficient β3 represents the vegetation resilience to drought, quantifying memory effects. A large value for β3 indicates that current season EVI strongly depends on previous states of the system and that the pastureland ecosystem recovers slowly from drought, and vice versa (see supporting information). The quadratic specification allows for a nonlinear relation in which maximum greenness (EVI) can occur at intermediate rates of precipitation. The cell-specific intercept (α_{is}) represents the effect of variables that vary across space for which observations are not available such as soil quality, nutrient availability, and temperature. Lagged values of precipitation are included because previous studies have found that grassland and semi-arid ecosystems respond to precipitation with time lags that range from 3 to 6 months (Lotsch et al., 2003; Sala et al., 2012; Vicente-Serrano et al., 2013). Lagged values of EVI are included

10.1029/2019EF001316

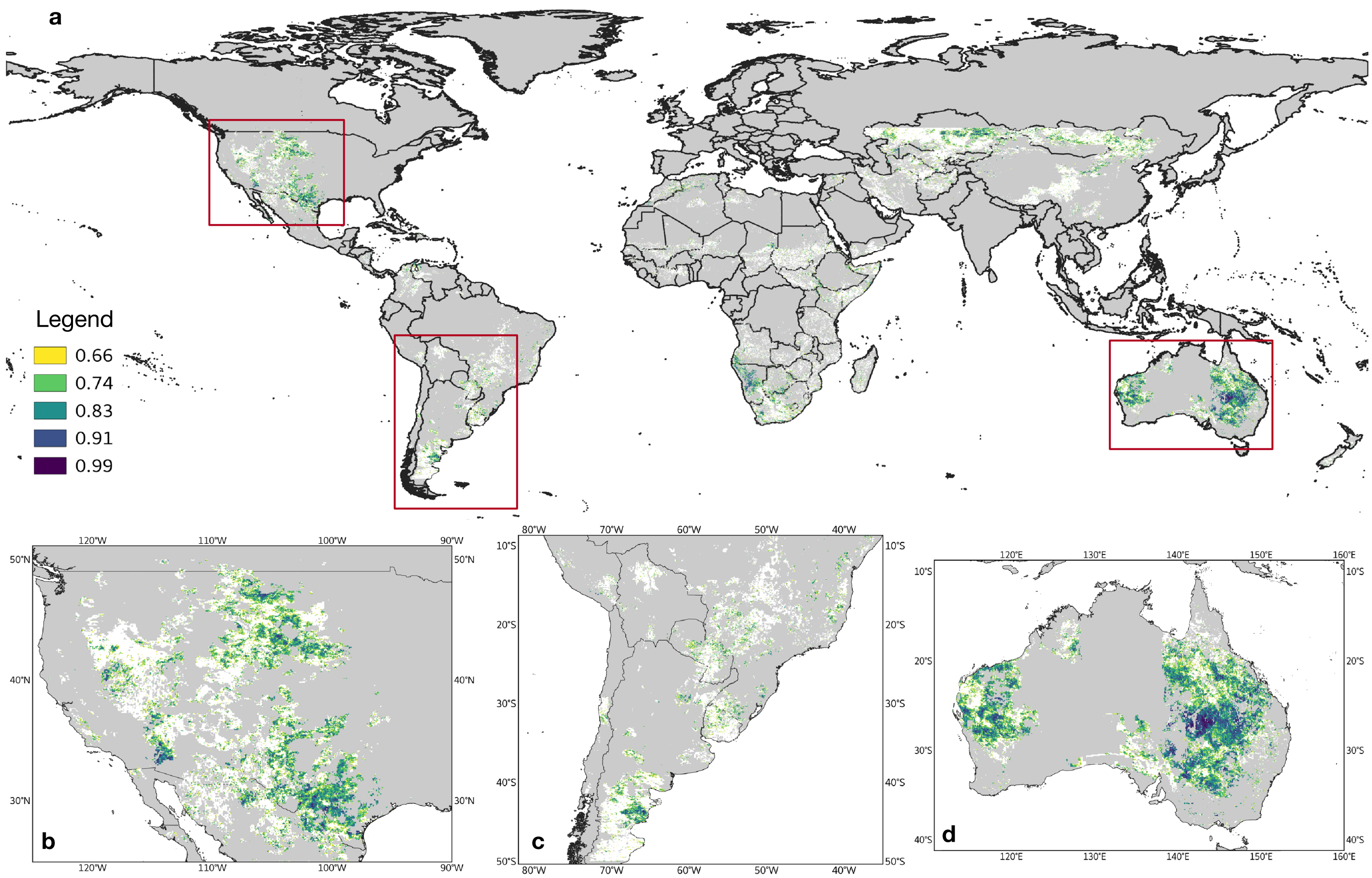

Figure 2. Grid cell R^2 values for statistically significant regression models ($p < 0.05$) for yearly precipitation and EVI anomalies, including lagged terms. Panel (a) shows global results, along with three specific pasturelands in regions of interest in the United States (b), Latin America (c), and Australia (d). White grid cells represent grid cells that do not show statistically significant R^2 values ($p < 0.05$). CHIRPS precipitation data are available between 50°S and 50°N, which is why pasturelands in Russia and Canada are excluded from the analysis.

because vegetation has "memory" such that its current state reflects the residual effects of previous conditions. For this work, we used a similar approach pursued in several previous studies that quantified resilience by measuring the time or rate of biomass recovery to a state that existed prior to disturbance (Tilman, 1996; Lhermitte et al., 2011; De Keersmaecker et al., 2015). Hence, this model considers standardized anomalies for both short-term precipitation effects and grassland system memory.

We use Equation (2) to characterize the response of vegetation greenness in global pasturelands to precipitation across 60 seasons (15 years) using the procedure developed by Swamy (1970). The model was estimated separately for each of the 20 study regions (Figure 1) by using all sample cells within each region together. We selected among models that are implied by four estimation techniques (pooled OLS, fixed effects, random effects, or random coefficient) using the model selection framework outlined in Zhou et al. (2003) (see supporting information). F tests indicated rejection of restrictions that make the intercepts and/or regression coefficients the same across grid cells. Finally, we evaluated whether the regression results were spurious by testing the null hypothesis that the dependent and independent variables contain a stochastic trend (Pedroni, 2001). We rejected this null hypothesis for all variables, which allowed us to proceed with the OLS framework. To quantify the effect of each independent variable on EVI anomalies, we simulated the regression model by holding three variables at their sample mean while allowing one variable (i.e., lagged EVI) to vary in a fashion that was consistent with historical observations. In this way, we assessed the relative contribution of precipitation and antecedent vegetation greenness to variability in vegetation greenness (Figure 3).

10.1029/2019EF001316

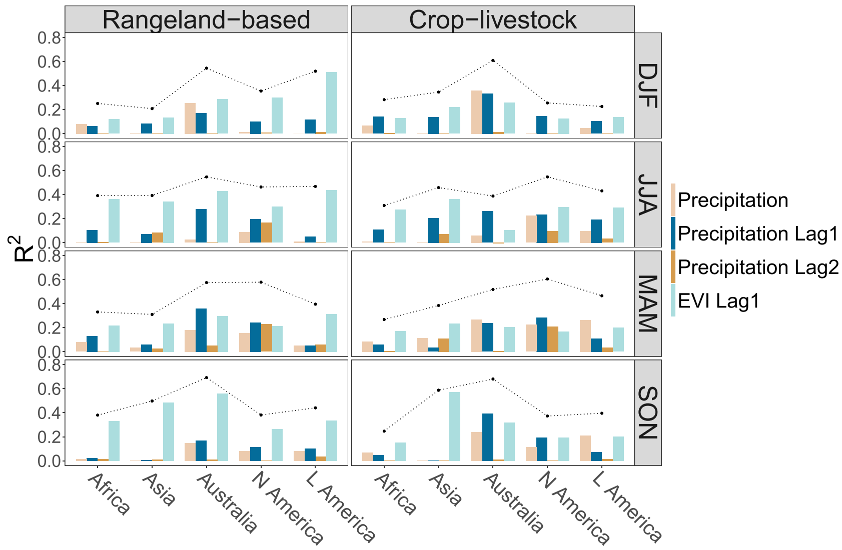

Figure 3. Partial R^2 values for each predictor variable in each region explaining variability in EVI anomalies in arid and semi-arid regions. The solid points above each production-region-season combination show the overall explanatory power of the model, and the colored bars show the contributions of contemporaneous and lagged precipitation and lagged EVI anomalies. Sample sizes in each region are provided in Table S1.

2.4. Asymmetry, Grid Cell Correlations, and Trends

Cell-wise regressions for all global pasturelands included in our analysis were calculated based on annual anomalies in precipitation and EVI. To quantify annual trends in EVI, we performed a Theil-Sen trend analysis for each cell by calculating the slopes of multiple randomized subsets of data generated via bootstrap resampling. The final Theil-Sen estimator is the median of all slopes and bootstrap resampling provides an estimate of the p value for the slope (Sen, 1968; Theil, 1950). Theil-Sen estimates are robust, resistant to outliers, and yield accurate confidence intervals (Sen, 1968; Theil, 1950). Lastly, we calculated the maximum positive and negative deviations from the long-term mean EVI (Knapp et al., 2017; Knapp & Smith, 2001). Following the methodology developed by Knapp and Smith (2001), we calculated maximum positive EVI deviations as $\frac{\text{max}-\text{mean}}{\text{mean}}$ and maximum negative EVI deviations as $\frac{\text{mean}-\text{min}}{\text{mean}}$. To test whether vegetation responds asymmetrically to precipitation above the sample mean, we multiplied the squared precipitation term in Equation (2) by a binary variable equal to one for seasons in which anomalies are positive and zero for seasons in which anomalies are negative.

3. Results

Results indicate widespread sensitivity of pastureland vegetation to both precipitation anomalies and short-term lagged vegetation anomalies. This sensitivity is most pronounced in arid and semi-arid regions where rangeland-based livestock production systems are the least resilient. As part of our analysis, we examined two key properties of pastureland response to precipitation: *engineering resilience*, which we define here as the time required for vegetation to recover following a disturbance, and *resistance*, which reflects the ability of pasturelands to withstand drought. As we indicate in section 2.3, lagged EVI is included in Equation (2) to quantify the importance and magnitude of lagged vegetation responses to variation in precipitation.

3.1. Annual Grid Cell Correlations and Trends

Globally, 28.3% of pasturelands show statistically significant correlations ($p < 0.05$) between vegetation index anomalies and current and antecedent precipitation anomalies as indicated by t statistics that reject the null hypothesis $\beta1 = 0$ or $\beta2 = 0$. More specifically, Figure 2 presents a map of the variance in EVI anomalies explained (R^2) by OLS regression models. Results from this analysis clearly show the geographic extent of pastureland sensitivity, with southwestern Africa, eastern Australia (Figure 2d), the Northern and Southern Great Plains of the United States (Figure 2b), parts of Eurasia, and Mongolia all showing strong sensitivity to precipitation anomalies. As expected, there is a strong correspondence between vegetation

10.1029/2019EF001316

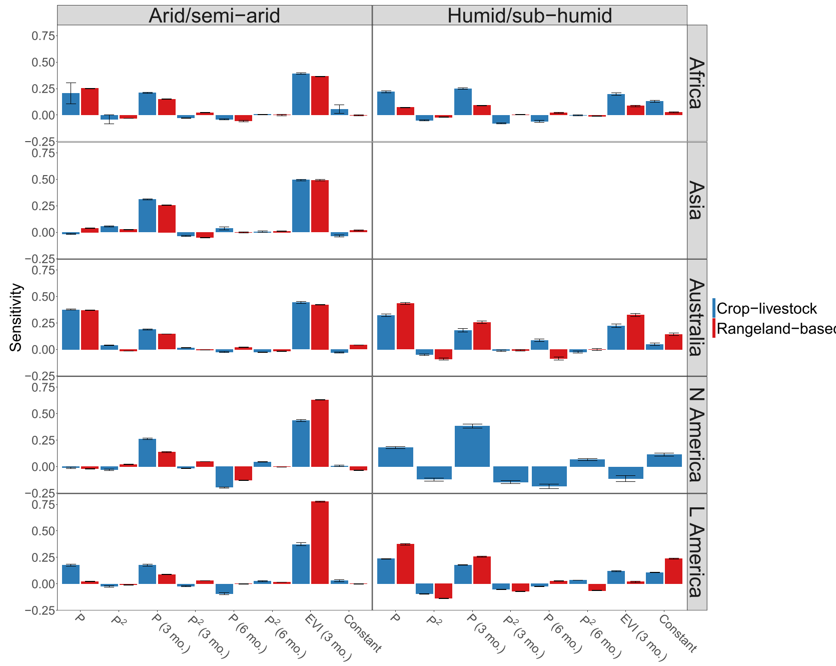

Figure 4. Sensitivity (change in EVI for a unit change in precipitation) of EVI anomalies to precipitation anomalies (P) for December/January/February (DJF); error bars represent one standard deviation. There were insufficient observations of pasturelands in humid Asia and in humid rangeland-based production systems in North America to estimate models for these strata. Sample sizes in each region are provided in Table S1.

dynamics and variation in precipitation in arid and semi-arid pasturelands, with 62.2% of statistically significant cells located in these climate zones. In this context, it is important to note that land management is not included in this part of the analysis (Figure 2). Hence, low correlation between vegetation dynamics and precipitation in some regions may reflect the role of human activities or other climate and edaphic factors that may limit growth.

While the majority of global pasturelands show no trend in overall greenness, 14.5% of global pastureland grid cells show statistically significant ($p < 0.05$) trends in EVI: 84.6% show greening and 15.4% show browning (Figure S6). Greening is most pronounced across arid and semi-arid pasturelands, where 79% of statistically significant Theil-Sen trends are positive. Trends in vegetation greenness between 2003 and 2017 show the largest magnitude (up to 0.10 EVI units total increase) over southeastern Australia, the northern Great Plains of the United States, Mato Grosso do Sul in Brazil, and in parts of China (Figure S6). This analysis also revealed statistically significant browning trends (up to −0.08 EVI units) over Kenya and Somalia in eastern Africa, and in Eastern Brazil in Latin America (Figure S6).

3.2. Seasonal Explanatory Power of Models and Predictors

To explore the magnitude of regional and seasonal patterns in the sensitivity of vegetation greenness anomalies to precipitation and antecedent greenness, we estimated the total and partial R^2 for each predictor variable in Equation (2) stratified by season, livestock production system, and region (Figure 3). In arid and semi-arid regions, anomalies in precipitation and lagged EVI accounted for 22% to 68% of total variation in seasonal EVI anomalies in crop-livestock systems and 20% to 69% of variation in seasonal EVI anomalies in rangeland-based systems. The magnitude of explained variance was particularly large in rangeland-based and crop-livestock systems in Australia, North America, and Latin America across all seasons and for arid crop-livestock systems in Australia (Figure 3). Importantly, lagged short-term vegetation greenness anomalies contributed at least a half of the explanatory power in most regions and seasons, with the exception of Australia and North America, where contemporaneous and short-term

10.1029/2019EF001316

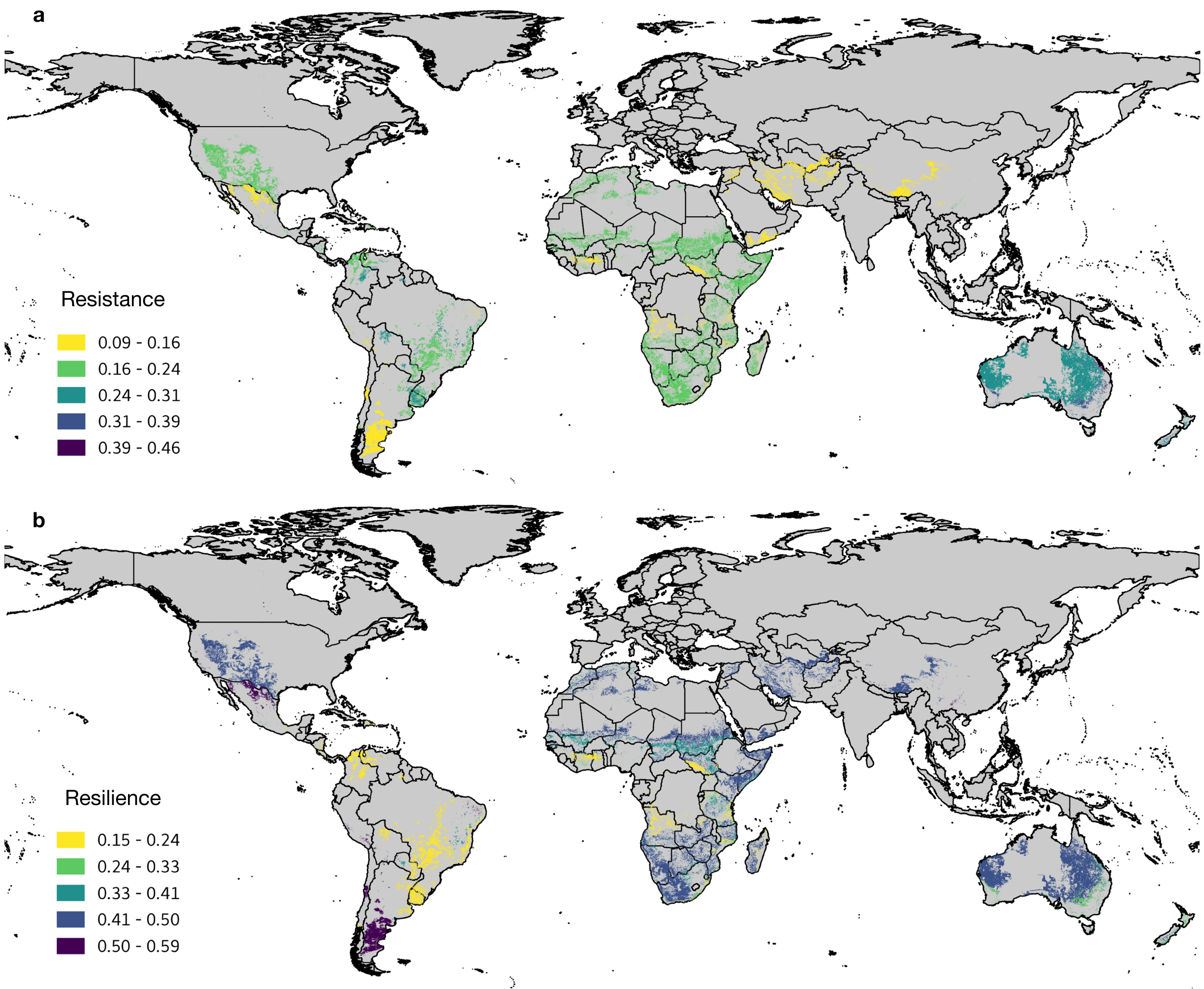

Figure 5. Global mean seasonal sensitivity of pasturelands: (a) resistance to drought and (b) resilience. This figure shows the model coefficients for precipitation (a) and lagged vegetation anomalies (b) for the 20 different study units. Higher numbers indicate lower resistance and resilience; that is, areas in purple and blue are most sensitive to change in precipitation regimes. Note that the two scales have different ranges.

precipitation anomalies explained a lot of the variability in greenness anomalies, especially in crop-livestock systems.

In humid and sub-humid climate zones, variation in precipitation and lagged EVI accounted for 16% to 69% and 5% to 72% of total variance in EVI anomalies across regions and seasons in crop-livestock systems and rangeland-based systems, respectively (Fig. S1). Lagged short-term vegetation greenness anomalies explain a smaller proportion of contemporaneous greenness in humid pasturelands than in arid and semi-arid pasturelands. Overall, the explanatory power of our models in humid and sub-humid pasturelands was smaller because of two main factors: (1) humid grasslands usually are not water limited, and (2) vegetation in humid pasturelands is more abundant (i.e., higher percent cover, leaf area, etc.) relative to vegetation in arid pasturelands. The explanatory power was particularly low in Africa and also in mixed crop-livestock production systems in all regions (Fig. S1).

Further analysis reveals geographic patterns in the statistically significant relationships ($p < 0.05$) between EVI anomalies and lagged anomalies in both precipitation and EVI. Specifically, there is a 3-month system memory, except in arid North American livestock production systems, where 6-month lagged precipitation anomalies account for nearly 20% of interannual variation in vegetation greenness anomalies during MAM and JJA (Figure 3). These results clearly indicate that dryland livestock production systems are sensitive

10.1029/2019EF001316

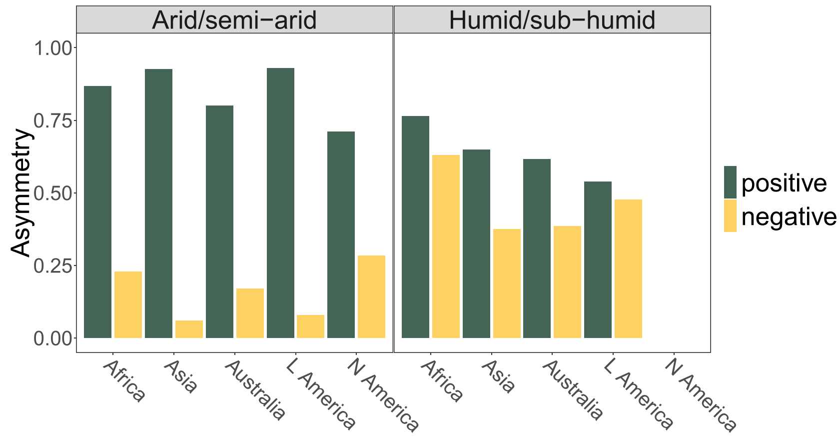

Figure 6. Maximum positive deviations from mean EVI are up to four times larger than the maximum negative deviations observed in the 15-year record in arid and semi-arid regions of the world. There were insufficient observations of pasturelands in humid systems in North America to estimate models for these strata. For sample size in each region please refer to Table S1.

to short-term (3-month lag) vegetation greenness anomalies (Figures 3 and 4). Specifically, livestock production systems in Australia are most sensitive (least resistant) to contemporaneous and short-term precipitation anomalies, while arid and semi-arid livestock production systems in Latin America are most sensitive (least resilient) to short-term vegetation greenness anomalies (Figures 3 and 4).

3.3. Seasonal Sensitivity of Pasturelands to Precipitation and Vegetation Anomalies

Pastureland EVI anomalies were positively correlated with both in-season and lagged precipitation anomalies across livestock production systems and agroecological zones. On average, above-average precipitation tended to increase vegetation greenness and below-average precipitation tended to decrease vegetation greenness (Figure 3). The magnitude of this effect depended on the location and climate regime. To illustrate, Figure 4 shows the sensitivity of EVI anomalies to variation in in-season and lagged precipitation anomalies (defined here as the unit change EVI for a unit change in precipitation, estimated based on the coefficients from Equation (2)), which can be related to pastureland stability. Specifically, the coefficients associated with precipitation ($\beta 1$ and $\beta 2$) capture the resistance of pasturelands to drought, and the coefficient associated with lagged EVI ($\beta 3$) captures the resilience of pasturelands to drought (or in other words the rate at which EVI adjusts to precipitation anomalies).

In arid and semi-arid regions, pasturelands were less sensitive to precipitation than short-term vegetation anomalies, which suggests that these regions are relatively resistant to drought, but have lower resilience once disturbed (Figure 4, Tables S3–S4). Conversely, humid and sub-humid pasturelands were less sensitive to short-term vegetation anomalies compared to arid and semi-arid regions, and as a result, pasturelands in these regions had greater resilience (Figure 4, Tables S3–S4).

In arid and semi-arid pasturelands, which were less resilient than humid and sub-humid pasturelands, rangeland-based and crop-livestock systems respond differently compared to one another (Figures S2–S4). Rangeland-based systems, which were more extensive, appear to be the least resilient. In particular, low resilience was pronounced in Africa, Australia, and Latin America during JJA and SON. Drought resistance, on the other hand, was relatively unaffected by the livestock production system or agroecological zone (Figures S2–S4). Inspection of the mean resistance and resilience across seasons reveals widespread sensitivity of pasturelands to precipitation and vegetation anomalies (Figure 5). Figure 5 shows the mean seasonal coefficients for precipitation anomalies (a) and vegetation anomalies (b) from Equation (2) across the 20 different study units. Low resilience (high value of $\beta 3$ coefficient) was found in arid and semi-arid areas and in particular in U.S. Southwest, Patagonia, southern Africa, the Sahel, and Australia (Figure 5b). Low drought resistance (high value of $\beta 1$ coefficient) was found in Australia, U.S. Southwest, Uruguay and parts of Brazil (Figure 5a). In particular, Australia had both low resistance and low resilience relative to other regions across the world. Patagonia, in southern South America, had the lowest resilience globally, which is indicative of slow vegetation recovery after disturbance (e.g., drought).

3.4. Asymmetry in the Response of Pastureland Greenness to Precipitation Anomalies

In the final element of our analysis we tested whether pastureland vegetation responds symmetrically to wet versus dry years. Results indicated that arid/semi-arid zones responded differently than humid/sub-humid zones, which suggests that biome-dependent factors, independent of precipitation, constrain the response of vegetation. In arid and semi-arid regions, maximum positive deviations in vegetation greenness were four times more numerous than maximum negative deviations (Figure 6). Although the same pattern is present in humid and sub-humid systems, differences in the magnitude of positive versus negative deviations is much smaller. Further, positive asymmetry in EVI response was not consistently explained by corresponding asymmetry in precipitation (Figure S5). To test whether asymmetry in the EVI response was explained by asymmetry in the magnitude of precipitation anomalies, we multiplied the squared precipitation term in Equation (2) by a binary variable (see methods for more details). Results from this analysis reveal that asymmetry in EVI response is not associated with differential response to wet versus dry years, except regionally in Latin America, Australia, and North America (Figure S5). For example, the positive EVI asymmetry in crop-livestock systems in Latin America is associated with wet years (on average $\beta 2 = 0.249$, $p < 0.05$). The lack of corresponding asymmetry in precipitation indicates that vegetation greenness can be influenced by other factors in addition to precipitation in the current season (i.e., antecedent precipitation and grazing intensity).

4. Discussion

This study provides a comprehensive analysis of the sensitivity of global pasturelands to change in precipitation across multiple agroecological zones and livestock production systems. Our results show that among those grid cells exhibiting statistically significant trends, 84.6% are greening (Figure S6), of which most are located in arid and semi-arid regions. These results are consistent with those from other studies showing that semi-arid regions of the Southern Hemisphere have experienced greening, especially in Australia, South America, and Southern Africa (Fensholt et al., 2012; Poulter et al., 2014). While the drivers behind this trend are unclear and likely vary by region, possible causes include changes in precipitation frequency and intensity (Donohue et al., 2009), woody encroachment as a result of livestock management (Andela et al., 2013; Asner et al., 2004), climate change (Maestre et al., 2016), and CO_2 fertilization (Zhu et al., 2016).

The resistance and resilience metrics used in this study are consistent with published ecosystem sensitivity metrics and provide effective and nuanced measures of how vegetation activity responds to variation in precipitation over short periods (i.e., 3 months) (De Keersmaecker et al., 2015; Vicente-Serrano et al., 2013). Our study finds that sensitivity to contemporaneous and short-term precipitation anomalies is highest (least resistance) in Australia across all combinations of agroecological zones and livestock production systems, while arid and semi-arid livestock production systems in Latin America are most sensitive (least resilient) to short-term vegetation greenness anomalies (Figure 4, Tables S3–S4). Field-based evidence suggests that low levels of plant density in arid and semi-arid grasslands of Latin America limit their ability to recover from the loss of vegetation associated with drought (e.g., Gaitán et al., 2014; Yahdjian & Sala, 2006). In this context, results from this study provide further empirical evidence regarding the importance of short-term vegetation anomalies as a major control on productivity in arid and semi-arid agroecological zones across the globe and in Latin America in particular. Specifically, vegetation in arid and semi-arid pasturelands is well-adapted to seasonal-scale precipitation deficits but highly responsive to disturbances in vegetation cover at interannual time scales caused by drought, for example.

While our results demonstrate the importance of precipitation as a key abiotic driver of variation and change in pasturelands, they also highlight that the rate of adjustment by vegetation to fluctuations in precipitation is low, indicating low resilience, and once perturbed, a slow return of the system to equilibrium. Moreover, the response of pastureland vegetation to climate forcing is also influenced by biotic factors such as grazing, which impacts the long-run productivity of pasturelands by changing the species composition and plant density (Briske et al., 2003; Fuhlendorf et al., 2001; Illius & O'Connor, 1999). Because the state and health of rangeland ecosystems reflect processes that include both equilibrium and nonequilibrium dynamics, both abiotic and biotic drivers such as those mentioned above can have long-term impacts on arid and semi-arid pasturelands by causing nonreversible changes in ecosystem state (Asner et al., 2004; Briske et al., 2003; Gaitán et al., 2014; Reynolds et al., 2007). Stated another way, maintaining and enhancing grassland cover in pasturelands by effective management of livestock can buffer the negative effects of climate variation on vegetation productivity and aid pasturelands in recovery from drought.

Finally, results from this study demonstrate that some pastureland systems show asymmetric response to precipitation anomalies (Knapp et al., 2015). This makes it difficult to predict the response of vegetation greenness to precipitation extremes based on the overall sensitivity of EVI to precipitation. Our results, which are based on remote sensing, are consistent with results from field studies: Maximum EVI values deviate more from the long-term mean than do minimum EVI values (Knapp & Smith, 2001; Knapp et al., 2017; Wu et al., 2015). Furthermore, statistical assessment of EVI dynamics demonstrates that crop-livestock systems in Latin America exhibit statistically significant asymmetric responses to wet versus dry years. The asymmetric response in vegetation greenness, however, may not always be a direct response to increased precipitation and can also reflect vegetation life history, legacy effects, or changes in plant communities. Even though wet years in arid regions can generate large pulses in productivity, the magnitude of the response is constrained by low plant density and leaf area (Huxman et al., 2004; Knapp & Smith, 2001). Consistent with this, our results suggest that in arid and semi-arid livestock production systems, pastureland greenness saturates during extremely wet seasons (Flombaum et al., 2017; Huxman et al., 2004; Yang et al., 2008; Zhou et al., 2003).

Pasturelands are globally extensive, sensitive to climate, and important both ecologically and socioeconomically. In the coming decades, as population growth and economic development increase the demand for meat and dairy products, pasturelands will experience increased stress from land use intensification and climate change. In this study, we used remote sensing, climate, and land use data to characterize and quantify the sensitivity of global pasturelands to the joint effects of climate variation and land use. Specifically, our analysis quantified the short-run effects of precipitation and vegetation anomalies on pastureland greenness across two agroecological zones and two broad classes of livestock production systems. Our results identify trends in pastureland greenness and sensitivity to climate and indicate how pasturelands located in existing dryland areas are likely to be affected by projected trends in precipitation. For example, browning in the Horn of Africa combined with sensitivity to drought and short-term vegetation anomalies make livestock production in this region particularly vulnerable to climate change and overgrazing.

5. Conclusions

Although some livestock producers may be able to adapt by implementing new strategies for dealing with declining carrying capacity for livestock in pasturelands (i.e., by using feed or moving herds to different ranges), others may be incapable of doing so because their grazing lands are already overgrazed (and hence are not able to recover from drought) or they do not have the means to adapt. While high livestock density in dryland pasturelands can reduce vegetation cover and grassland species diversity, appropriate management can also be effective in supporting and maintaining healthy vegetation and productive vegetation stocks. By stratifying our analysis into different livestock production systems, we separate land areas that are most likely to experience degradation from those that are more likely to maintain their ability to support livestock. Our results suggest that globally, regions most likely to experience degradation include arid and semi-arid rangeland-based systems located in Australia and Latin America. These two regions exhibited the lowest resilience and drought resistance, which means they not only struggle to recover from disturbance, but they are also vulnerable to state transitions. More generally, our results show that large swaths of semi-arid global pasturelands have substantial sensitivity to variation in precipitation and, hence, are vulnerable to climate change. Moving forward, improved climate model projections in combination with operational monitoring systems, perhaps building off the framework we used for this work, will be required to support and ensure effective management of both regional and global land use in pasturelands.

Acknowledgments

This research was developed in part during the Young Scientists Summer Program at the International Institute for Applied Systems Analysis, Laxenburg, Austria, with financial support from the U.S. National Member Organization. This work was supported by NASA Headquarters under the NASA Earth and Space Science Fellowship Program - Grant 80NSSC17K0378. The authors declare no conflict of interest. The Climate Hazards Group InfraRed Precipitation Station (CHIRPS) data were retrieved from ftp://ftp.chg.ucsb.edu/pub/org/chg/products/CHIRPS-2.0/global_monthly_EWX/data/. The Collection 6 MODIS monthly EVI data (MOD13C2) data were retrieved from https://e4ftl01.cr.usgs.gov//MODV6_Cmp_C/MOLT/MOD13C2.006/. The pastureland extent map produced by Ramankutty et al. (2008) was retrieved from http://www.earthstat.org/cropland-pasture-area-2000/. Lastly, data on agroecological zones and livestock production systems were downloaded from the Food and Agriculture Organization's website (http://www.fao.org/livestock-systems/production-systems/en/). The data sets used in this analysis are available from their respective sources linked above. Data produced in this study are available in the following repository: https://open.bu.edu/handle/2144/36592.

References

Andela, N., Liu, Y. Y., van Dijk, A. I. J. M., de Jeu, R. A. M., & McVicar, T. R. (2013). Global changes in dryland vegetation dynamics (1988–2008) assessed by satellite remote sensing: Comparing a new passive microwave vegetation density record with reflective greenness data. *Biogeosciences*, *10*, 6657–6676.

Arnone, J. A. III, Verburg, P. S. J., Johnson, D. W., Larsen, J. D., Jasoni, R. L., Lucchesi, A. J., et al. (2008). Prolonged suppression of ecosystem carbon dioxide uptake after an anomalously warm year. *Nature*, *455*(7211), 383–386. https://doi.org/10.1038/nature07296
Asner, G. P., Elmore, A. J., Olander, L. P., Martin, R. E., & Harris, A. T. (2004). Grazing systems, ecosystem responses, and global change. *Annual Review of Environment and Resources*, *29*(1), 261–299.
Asrar, G., Fuchs, M., Kanemasu, E. T., & Hatfield, J. L. (1984). Estimating absorbed photosynthetic radiation and leaf area index from spectral reflectance in wheat. *Agronomy Journal*, *76*(2), 300–306.
Briske, D. D., Fuhlendorf, S. D., & Smeins, F. E. (2003). Vegetation dynamics on rangelands: A critique of the current paradigms. *Journal of Applied Ecology*, *40*(4), 601–614.
Bunting, E. L., Munson, S. M., & Villarreal, M. L. (2017). Climate legacy and lag effects on dryland plant communities in the southwestern U.S. *Ecological Indicators*, *74*, 216–229.
De Keersmaecker, W., Lhermitte, S., Tits, L., Honnay, O., Somers, B., & Coppin, P. (2015). A model quantifying global vegetation resistance and resilience to short-term climate anomalies and their relationship with vegetation cover: Global vegetation resistance and resilience. *Global Ecology and Biogeography*, *24*(5), 539–548.
Del Grosso, S., Parton, W., Stohlgren, T., Zheng, D., Bachelet, D., Prince, S., et al. (2008). Global potential net primary production predicted from vegetation class, precipitation, and temperature. *Ecology*, *89*(8), 2117–2126. https://doi.org/10.1890/07-0850.1
Didan, K. (2015). MOD13C2 MODIS/Terra Vegetation Indices Monthly L3 Global 0.05Deg CMG V006 [Data set]. NASA EOSDIS LP DAAC. https://doi.org/10.5067/MODIS/MOD13C2.006
Donohue, R. J., McVicar, T. R., & Roderick, M. L. (2009). Climate-related trends in Australian vegetation cover as inferred from satellite observations, 1981-2006. *Global Change Biology*, *15*(4), 1025–1039.
Ellis, J. E., & Swift, D. M. (1988). Stability of African pastoral ecosystems: Alternate paradigms and implications for development. *Journal of Range Management*, *41*(6), 450.
Fensholt, R., Langanke, T., Rasmussen, K., Reenberg, A., Prince, S. D., Tucker, C., et al. (2012). Greenness in semi-arid areas across the globe 1981–2007—An Earth Observing Satellite based analysis of trends and drivers. *Remote Sensing of Environment*, *121*, 144–158. https://doi.org/10.1016/j.rse.2012.01.017
Fernandez-Gimenez, M. E., & Allen-Diaz, B. (1999). Testing a non-equilibrium model of rangeland vegetation dynamics in Mongolia. *Journal of Applied Ecology*, *36*(6), 871–885.
Fetzel, T., Havlik, P., Herrero, M., Kaplan, J. O., Kastner, T., Kroisleitner, C., et al. (2017). Quantification of uncertainties in global grazing systems assessment. *Global Biogeochemical Cycles*, *31*, 1089–1102. https://doi.org/10.1002/2016GB005601
Flombaum, P., Yahdjian, L., & Sala, O. E. (2017). Global-change drivers of ecosystem functioning modulated by natural variability and saturating responses. *Global Change Biology*, *23*(2), 503–511. https://doi.org/10.1111/gcb.13441
Foley, J. A., Ramankutty, N., Brauman, K. A., Cassidy, E. S., Gerber, J. S., Johnston, M., et al. (2011). Solutions for a cultivated planet. *Nature*, *478*(7369), 337–342. https://doi.org/10.1038/nature10452
Friedl, M. A., Sulla-Menashe, D., Tan, B., Schneider, A., Ramankutty, N., Sibley, A., & Huang, X. (2010). MODIS Collection 5 global land cover: Algorithm refinements and characterization of new datasets. *Remote Sensing of Environment*, *114*(1), 168–182.
Fuhlendorf, S. D., Briske, D. D., & Smeins, F. E. (2001). Herbaceous vegetation change in variable rangeland environments: The relative contribution of grazing and climatic variability. *Applied Vegetation Science*, *4*(2), 177–188.
Funk, C., Peterson, P., Landsfeld, M., Pedreros, D., Verdin, J., Shukla, S., et al. (2015). The climate hazards infrared precipitation with stations—A new environmental record for monitoring extremes. *Scientific Data*, *2*(1), 150066. https://doi.org/10.1038/sdata.2015.66
Funk, C., Verdin, A., Michaelsen, J., Peterson, P., Pedreros, D., & Husak, G. (2015). A global satellite-assisted precipitation climatology. *Earth System Science Data*, *7*, 275–287.
Gaitán, J. J., Oliva, G. E., Bran, D. E., Maestre, F. T., Aguiar, M. R., Jobbágy, E. G., et al. (2014). Vegetation structure is as important as climate for explaining ecosystem function across Patagonian rangelands. *Journal of Ecology*, *102*(6), 1419–1428. https://doi.org/10.1111/1365-2745.12273
Guo, Q., Hu, Z., Li, S., Li, X., Sun, X., & Yu, G. (2012). Spatial variations in aboveground net primary productivity along a climate gradient in Eurasian temperate grassland: Effects of mean annual precipitation and its seasonal distribution. *Global Change Biology*, *18*(12), 3624–3631.
Hansen, J., Ruedy, R., Glascoe, J., & Sato, M. (1999). GISS analysis of surface temperature change. *Journal of Geophysical Research*, *104*(D24), 30997–31022.
Herrero, M., Havlik, P., Valin, H., Notenbaert, A., Rufino, M. C., Thornton, P. K., et al. (2013). Biomass use, production, feed efficiencies, and greenhouse gas emissions from global livestock systems. *Proceedings of the National Academy of Sciences*, *110*(52), 20888–20893. https://doi.org/10.1073/pnas.1308149110
Hsiao, C. (2014). *Analysis of panel data*, (3rd ed.). Cambridge: Cambridge University Press.
Huang, J., Yu, H., Guan, X., Wang, G., & Guo, R. (2015). Accelerated dryland expansion under climate change. *Nature Climate Change*, *6*, 166–171.
Huxman, T. E., Smith, M. D., Fay, P. A., Knapp, A. K., Shaw, M. R., Loik, M. E., et al. (2004). Convergence across biomes to a common rain-use efficiency. *Nature*, *429*(6992), 649–651.
Illius, A. W., & O'Connor, T. G. (1999). On the relevance of nonequilibrium concepts to arid and semiarid grazing systems. *Ecological Applications*, *9*(3), 798–813.
Keesstra, S. D., Bouma, J., Wallinga, J., Tittonell, P., Smith, P., Cerdà, A., et al. (2016). The significance of soils and soil science towards realization of the United Nations Sustainable Development Goals. *The Soil*, *2*(2), 111–128. https://doi.org/10.5194/soil-2-111-2016
Knapp, A. K., Ciais, P., & Smith, M. D. (2017). Reconciling inconsistencies in precipitation-productivity relationships: Implications for climate change. *New Phytologist*, *214*(1), 41–47. https://doi.org/10.1111/nph.14381
Knapp, A. K., Hoover, D. L., Wilcox, K. R., Avolio, M. L., Koerner, S. E., La Pierre, K. J., et al. (2015). Characterizing differences in precipitation regimes of extreme wet and dry years: Implications for climate change experiments. *Global Change Biology*, *21*(7), 2624–2633. https://doi.org/10.1111/gcb.12888
Knapp, A. K., & Smith, M. D. (2001). Variation among biomes in temporal dynamics of aboveground primary production. *Science*, *291*(5503), 481–484. https://doi.org/10.1126/science.291.5503.481
Lhermitte, S., Verbesselt, J., Verstraeten, W. W., Veraverbeke, S., & Coppin, P. (2011). Assessing intra-annual vegetation regrowth after fire using the pixel based regeneration index. *ISPRS Journal of Photogrammetry and Remote Sensing*, *66*(1), 17–27.
Lobell, D. B., & Burke, M. B. (2010). On the use of statistical models to predict crop yield responses to climate change. *Agricultural and Forest Meteorology*, *150*(11), 1443–1452.

Lotsch, A., Friedl, M. A., Anderson, B. T., & Tucker, C. J. (2003). Coupled vegetation-precipitation variability observed from satellite and climate records: Vegetation-precipitation dynamics. *Geophysical Research Letters*, *30*(14), 1774. https://doi.org/10.1029/2003GL017506

Maestre, F. T., Eldridge, D. J., Soliveres, S., Kéfi, S., Delgado-Baquerizo, M., Bowker, M. A., et al. (2016). Structure and Functioning of Dryland Ecosystems in a Changing World. *Annual Review of Ecology, Evolution, and Systematics*, *47*(1), 215–237. https://doi.org/10.1146/annurev-ecolsys-121415-032311

Myneni, R. B., Hall, F. G., Sellers, P. J., & Marshak, A. L. (1995). The interpretation of spectral vegetation indexes. *IEEE Transactions on Geoscience and Remote Sensing*, *33*(2), 481–486.

Pedroni, P. (2001). Purchasing power parity tests in cointegrated panels. *Review of Economics and Statistics*, *83*(4), 727–731.

Poulter, B., Frank, D., Ciais, P., Myneni, R. B., Andela, N., Bi, J., et al. (2014). Contribution of semi-arid ecosystems to interannual variability of the global carbon cycle. *Nature*, *509*(7502), 600–603. https://doi.org/10.1038/nature13376

Ramankutty, N., Evan, A. T., Monfreda, C., & Foley, J. A. (2008). Farming the planet: 1. Geographic distribution of global agricultural lands in the year 2000: Global agricultural lands in 2000. *Global Biogeochemical Cycles*, *22*, GB1003. https://doi.org/10.1029/2007GB002952

Ramankutty, N., Foley, J. A., Norman, J., & Mcsweeny, K. (2002). The global distribution of cultivable lands: Current patterns and sensitivity to possible climate change. *Global Ecology and Biogeography*, *11*, 377–392.

Reeves, M. C., Moreno, A. L., Bagne, K. E., & Running, S. W. (2014). Estimating climate change effects on net primary production of rangelands in the United States. *Climatic Change*, *126*(3–4), 429–442.

Reynolds, J. F., Smith, D. M. S., Lambin, E. F., Turner, B. L., Mortimore, M., Batterbury, S. P. J., et al. (2007). Global desertification: Building a science for dryland development. *Science*, *316*(5826), 847–851. https://doi.org/10.1126/science.1131634

Robinson, T., Thornton, P., Franceschini, G., Kruska, R., Chiozza, F., Notenbaert, A., et al. (2011). Global livestock production systems. Food and Agriculture Organization of the United Nations (FAO) and International Livestock Research Institute (ILRI).

Robinson, T.P., Thornton P., Franceschini G., Kruska R., Chiozza, F., Notenbaert, A., et al. (2018). Global distribution of ruminant livestock production systems V5 (5 minutes arc). Harvard Database V1

Sala, O. E., Gherardi, L. A., Reichmann, L., Jobbagy, E., & Peters, D. (2012). Legacies of precipitation fluctuations on primary production: theory and data synthesis. *Philosophical Transactions of the Royal Society, B: Biological Sciences*, *367*(1606), 3135–3144.

Sala, O. E., Parton, W. J., Joyce, L. A., & Lauenroth, W. K. (1988). Primary production of the central grassland region of the United States. *Ecology*, *69*(1), 40–45.

Seddon, A. W. R., Macias-Fauria, M., Long, P. R., Benz, D., & Willis, K. J. (2016). Sensitivity of global terrestrial ecosystems to climate variability. *Nature*, *531*(7593), 229–232. https://doi.org/10.1038/nature16986

Sen, P. K. (1968). Robustness of some nonparametric procedures in linear modes. *The Annals of Mathematical Studies*, *39*(6), 1913–1922.

Steinfeld, H., & Gerber, P. (2010). Livestock production and the global environment: Consume less or produce better? *Proceedings of the National Academy of Sciences*, *107*(43), 18237–18238.

Sulla-Menashe, D., Gray, J. M., Abercrombie, P. S., & Friedl, M. A. (2019). Hierarchical mapping of annual global land cover 2001 to present: The MODIS Collection 6 Land Cover product. *Remote Sensing of Environment*. *222*, 183–194. https://doi.org/10.1016/j.rse.2018.12.013

Swamy, P. A. V. B. (1970). Efficient inference in a random coefficient regression model. *Econometrica*, *38*(2), 311.

Theil, H. (1950). A rank-invariant method of linear and polynomial regression analysis. *Proceedings of Koninklijke Nederlandse Akademie van Wetenschappen*, 1397–1412.

Tilman, D. (1996). Biodiversity: Population Versus Ecosystem Stability. *Ecology*, *77*(2), 350–363.

Vicente-Serrano, S. M., Gouveia, C., Camarero, J. J., Begueria, S., Trigo, R., Lopez-Moreno, J. I., et al. (2013). Response of vegetation to drought time-scales across global land biomes. *Proceedings of the National Academy of Sciences*. *110*(1), 52–57. https://doi.org/10.1073/pnas.1207068110

Wang, L., D'Odorico, P., Evans, J. P., Eldridge, D., McCabe, M. F., Caylor, K. K., & King, E. G. (2012). Dryland ecohydrology and climate change: Critical issues and technical advances. *Hydrology and Earth System Sciences Discussions*, *9*(4), 4777–4825.

Wilcox, K. R., Shi, Z., Gherardi, L. A., Lemoine, N. P., Koerner, S. E., Hoover, D. L., et al. (2017). Asymmetric responses of primary productivity to precipitation extremes: A synthesis of grassland precipitation manipulation experiments. *Global Change Biology*, *23*(10), 4376–4385. https://doi.org/10.1111/gcb.13706

Wu, D., Zhao, X., Liang, S., Zhou, T., Huang, K., Tang, B., & Zhao, W. (2015). Time-lag effects of global vegetation responses to climate change. *Global Change Biology*, *21*(9), 3520–3531. https://doi.org/10.1111/gcb.12945

Yahdjian, L., & Sala, O. E. (2006). Vegetation structure constrains primary production response to water availability in the Patagonian steppe. *Ecology*, *87*(4), 952–962. https://doi.org/10.1890/0012-9658(2006)87[952:vscppr]2.0.co;2

Yang, Y., Fang, J., Ma, W., & Wang, W. (2008). Relationship between variability in aboveground net primary production and precipitation in global grasslands. *Geophysical Research Letters*, *35*, L23710. https://doi.org/10.1029/2008GL035408

Zhou, L., Kaufmann, R. K., Tian, Y., Myneni, R. B., & Tucker, C. J. (2003). Relation between interannual variations in satellite measures of northern forest greenness and climate between 1982 and 1999. *Journal of Geophysical Research*, *108*(D1), 4004. https://doi.org/10.1029/2002JD002510

Zhu, Z., Piao, S., Myneni, R. B., Huang, M., Zeng, Z., Canadell, J. G., et al. (2016). Greening of the Earth and its drivers. *Nature Climate Change*, *6*(8), 791–795. https://doi.org/10.1038/nclimate3004